SPECIAL TOPIC — Smart design of materials and design of smart materials

Reconstruction and stability of Fe_3O_4 (001) surface: An investigation based on particle swarm optimization and machine learning

Hongsheng Liu(柳洪盛), Yuanyuan Zhao(赵圆圆), Shi Qiu(邱实), Jijun Zhao(赵纪军), and Junfeng Gao(高峻峰)[†]

Key Laboratory of Materials Modification by Laser, Ion and Electron Beams (Dalian University of Technology), Ministry of Education, Dalian 116024, *China*

(Received 15 January 2023; revised manuscript received 2 February 2023; accepted manuscript online 8 February 2023)

Magnetite nanoparticles show promising applications in drug delivery, catalysis, and spintronics. The surface of magnetite plays an important role in these applications. Therefore, it is critical to understand the surface structure of Fe_3O_4 at atomic scale. Here, using a combination of first-principles calculations, particle swarm optimization (PSO) method and machine learning, we investigate the possible reconstruction and stability of Fe_3O_4(001) surface. The results show that besides the subsurface cation vacancy (SCV) reconstruction, an A layer with Fe vacancy (A-layer-V_{Fe}) reconstruction of the (001) surface also shows very low surface energy especially at oxygen poor condition. Molecular dynamics simulation based on the iron–oxygen interaction potential function fitted by machine learning further confirms the thermodynamic stability of the A-layer-V_{Fe} reconstruction. Our results are also instructive for the study of surface reconstruction of other metal oxides.

Keywords: surface reconstruction, magnetite surface, particle swarm optimization, machine learning

PACS: 68.35.–p, 68.35.B– **DOI:** 10.1088/1674-1056/acb9e4

1. Introduction

Surface reconstruction has significant influence on physical and chemical properties of materials. Usually, multi-component materials, like transition metal oxides undergo complex surface reconstruction. Magnetite (Fe_3O_4) attracts increasing attention due to its promising application in nanomedicine,[1–5] spintronics,[6,7] and catalysis.[8,9]

At room temperature, magnetite crystallizes in an inverse spinel structure with oxygen anions arranged in a slightly distorted face centered cubic lattice and iron atoms occupying tetrahedral and octahedral interstitial sites. Magnetite is ferrimagnetic with a Curie temperature as high as 858 K. The electronic properties of magnetite are still under debate and a recent hybrid functional study suggests that above Verwey temperature[10] bulk magnetite is a semiconductor with a small band gap.[11]

The (001) surface is one of the most important low-index facets of Fe_3O_4. Because of the complexity of the surface reconstruction, the atomic structure of Fe_3O_4 (001) surface has been investigated for more than 30 years both theoretically and experimentally.[12–22] Along the [001] direction, magnetite can be viewed as alternative stacking of A layers and B layers. A layer is made of tetrahedral iron (Fe_{Tet}) and B layer is composed of both oxygen and octahedral iron (Fe_{Oct}). Scanning tunneling microscopy (STM) images in experiments suggest a $(\sqrt{2}\times\sqrt{2})R45^\circ$ reconstruction of the Fe_3O_4 (001) surface.[13–18] Based on the STM observation, several atomic structure models have been proposed for the (001) surface.[14–20] Both A layer termination and B layer termination together with possible Fe and oxygen vacancies were considered in the early proposed models.[14–18] In 2005, a distorted bulk truncation (DBT) model was proposed, which shown higher thermodynamical stability than the early models.[19] However, the adsorption behavior of Au adatoms on the (001) surface cannot be explained based on the DBT model.[20–23] In 2014, a subsurface cation vacancy (SCV) model with interstitial Fe_{Tet} atom in the second layer and Fe_{Oct} vacancies in the third layer was proposed.[20] Density functional theory calculations show that the SCV model is more stable than DBT model at a large range of oxygen chemical potentials and the simulated STM agrees well with experimental STM. Moreover, based on the SCV model, the adsorption behavior of Au adatoms on the (001) surface can be well understood.[20]

However, up to now, from the theoretical side, the prediction and confirmation of the atomic structure of Fe_3O_4 (001) surface is only based on density functional theory (DFT) study, which is usually precise but limited in both model size and finite temperature simulation. A powerful theoretical prediction and a finite temperature simulation at a larger scale is expected to further confirm the surface reconstruction and stability. Recently, the particle swarm optimization (PSO) and the machine learning methods show powerful ability in materials design.[24–30] In this paper, combined DFT calculations, PSO method and machine learning method, the reconstruction and stability of Fe_3O_4 (001) surface are fully investigated. Our

[†]Corresponding author. E-mail: gaojf@dlut.edu.cn

© 2023 Chinese Physical Society and IOP Publishing Ltd

results show that A layer with Fe vacancy (A-layer-V_{Fe}) reconstruction of the (001) surface is a stable surface and is the most stable one at a poor oxygen condition. Machine learning works well for iron oxides and the molecular dynamics simulation based on machine learning iron-oxygen interaction potential further confirms the thermodynamic stability of the A-layer-V_{Fe} reconstruction.

2. Methods

The DFT calculations were carried out using the Vienna *Ab-initio* Simulation Package (VASP).[31] Projector augmented wave (PAW) potentials[32] were used to describe electron–ion interactions. The Perdew–Burke–Ernzerhof (PBE) functional within the generalized gradient approximation (GGA)[33] was adopted. A kinetic energy cutoff of 450 eV for the planewave basis, a convergence criterion of 10^{-4} eV for the total energy and a convergence criterion of 0.02 eV/Å for the force on each atom were adopted. To properly deal with the strong correlation effects among Fe 3d electrons, an on-site Coulomb correction with an effective U–J value of 3.5 eV was adopted according to our previous work on magnetite bulk[11] and surface.[22]

CALYPSO code was used to search stable structures of the (001) surface. A $(\sqrt{2}\times\sqrt{2})$ supercell for the (001) surface was used for different models because the Fe_3O_4 (001) surface shows a $(\sqrt{2}\times\sqrt{2})$ period according to STM images in experiments.[13–18] In the z direction a vacuum of more than 12 Å was introduced to avoid the spurious interaction between periodic images. Different termination and different Fe/O ratio on the surface were considered. During the PSO searching, it is not possible to keep the models symmetric at the moment. Therefore, during the PSO searching, asymmetrical slab models with bottom layers fixed to their bulk positions were used. The low-coordinated oxygen and iron atoms were saturated by H atoms. Then, after PSO searching, symmetric slab models were constructed followed by DFT geometry optimization. The number of layers in the symmetric slab models is more than fifteen. During geometry optimization, five layers in the middle are fixed to the bulk positions. For each termination and Fe/O ratio, 30 initial structures were randomly generated followed by DFT geometry optimization. According to the calculated total energy, the lower 60% of structures are used to generate the next generation of structures through the PSO method. 40% of structures for the next generation are randomly generated. Each generation produces 30 structures and a total of 5 generations are calculated.

To explore the thermodynamic stability of surface reconstruction at a larger scale, we fitted the Fe–O interaction potential by machine learning. Using the atomic centrosymmetric function,[34] the neural network is constructed by aenet (the atomic energy network) software package. The method splits the total energy of the structure into the sum of the energy of each atom. Therefore, the input of the neural network is first constructed by using the weighted radial distribution function (RDF) and the angular distribution function (ADF) to describe the chemical environment around the atom[35] as

$$\mathrm{RDF}_i(r)=\sum\delta(r-R_{ij})\,f_{\mathrm{c}}(R_{ij})\,\omega_{t_j}, \tag{1}$$

$$\mathrm{ADF}_i(\theta)=\sum\delta\left(\theta-\theta_{ijk}\right)f_{\mathrm{c}}(R_{ij})\,f_{\mathrm{c}}(R_{ik})\,\omega_{t_j}\omega_{t_k}, \tag{2}$$

where, i, j, k represents different atoms, R_{ij}, R_{ik} represents the distance between different atoms, θ_{ijk} is the angle between the three atoms of i, j, k, ω is the weight coefficient, representing different atomic species, $f_{\mathrm{c}}(r)=0.5\left(\cos\left(r\pi/R_{\mathrm{c}}\right)\right)$, R_{c} is the cutoff radius. In order to facilitate the input of the neural network, the first Chebyshev polynomial is used to expand the above two distribution functions as

$$C_{\mathrm{R}}^{n}=\sum\phi(R_{ij})\,f_{\mathrm{c}}(R_{ij})\,\omega_{t_j}, \tag{3}$$

$$C_{\mathrm{A}}^{n}=\sum\phi\left(\theta_{ijk}\right)f_{\mathrm{c}}(R_{ij})\,f_{\mathrm{c}}(R_{ik})\,\omega_{t_j}\omega_{t_k}. \tag{4}$$

Finally, the $N_{\mathrm{R}}+N_{\mathrm{A}}$ first Chebyshev polynomial is used as the basis function as the input layer of the neural network, the hyperbolic tangent function is used as the activation function of the hidden layer, and the double hidden layer (10-10) is used to construct the neural network. The output layer contains only one neuron, representing the energy contribution of the atom. The total energy is $E_{\mathrm{total}}=\sum^{N_{\mathrm{atom}}}E_i$.

Utilizing the machine learning Fe–O interaction potential, NVT molecular dynamics (MD) simulations at 400 K were performed with LAMMPS code for the A-layer-V_{Fe} (001) surface model with a (3×3) supercell. A timestep of 1 fs was used for the MD simulation.

3. Results and discussion

To search stable structures of the Fe_3O_4 (001) surface, different surface termination with possible iron or oxygen vacancies was considered. For a given termination and Fe/O ratio, large number of structures were created randomly. Then PSO method implemented in the CALYPSO code was used to search the most stable structure at the given termination and Fe/O ratio. Several structures in relative low energy, including the SCV,[20] DBT,[19] A-layer, reconstructed A-layer, A-layer with one Fe vacancy per $(\sqrt{2}\times\sqrt{2})$ supercell (A-layer-V_{Fe}), A-layer with one Fe adatom per $(\sqrt{2}\times\sqrt{2})$ supercell (A-layer-Fe adatom), B-layer with one oxygen vacancy per $(\sqrt{2}\times\sqrt{2})$ supercell (B-layer-V_O-1 and B-layer-V_O-2) and B-layer with one Fe vacancy per $(\sqrt{2}\times\sqrt{2})$ supercell (B-layer-V_{Fe}) were obtained after five generation of PSO searching. Here, A-layer and B-layer refer to tetrahedral Fe (Fe_{Tet}) layer and octahedral Fe (Fe_{Oct}) layer terminated surfaces, respectively.

To estimate and compare the stability of different surface models, surface energy γ was calculated as a function of chemical potential of oxygen:[36]

$$\gamma = \frac{1}{2A}\left[E_{\text{total}} - \frac{1}{3}N_{\text{Fe}}E_{\text{Fe}_3\text{O}_4} + \left(\frac{4}{3}N_{\text{Fe}} - N_{\text{O}}\right)\mu_{\text{O}}\right], \quad (5)$$

where, A is the surface area of the $(\sqrt{2}\times\sqrt{2})R45^\circ$ supercell, E_{total} is the total energy of the slab model and $E_{\text{Fe}_3\text{O}_4}$ is the total energy of bulk Fe_3O_4 per formula unit. μ_{O} is the chemical potential of oxygen. N_{Fe} and N_{O} are the numbers of Fe and oxygen atoms, respectively. According to formula (5), surface energies for selective surface models are plotted and shown in Fig. 1, where the zero reference for the chemical potential of oxygen is half the total energy of an isolated O_2 molecule. At a large range of μ_{O}, SCV model is the most stable surface. Besides the stable SCV and DBT models proposed before, we find that the A-layer-V_{Fe} model is also a very stable surface. At a very poor O_2 condition, the A-layer-V_{Fe} model becomes the most stable structure.

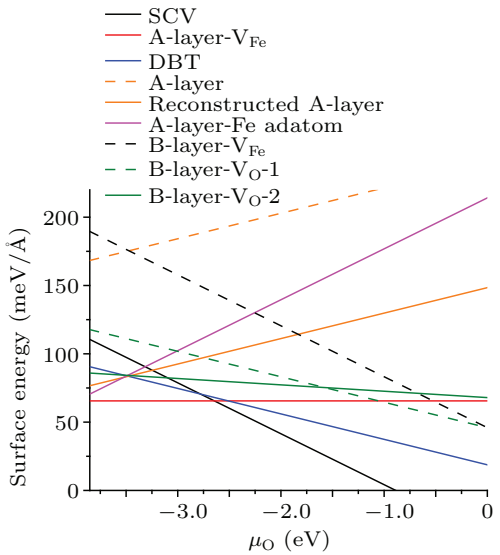


Fig. 1. Calculated surface free energy as a function of the chemical potential of oxygen for selected surface models.

The relative stability of the Fe_3O_4 surface depends on the environmental conditions. For example, previous study shows that with proper water adsorption, the DBT surface can be more stable than the SCV surface.[22] Therefore, the A-layer-V_{Fe} surface may exist under proper conditions. The atomic structure of the A-layer-V_{Fe} model is shown in Fig. 2. After geometry optimization, the iron atoms in the original top A layer (green balls on the top layer in Fig. 2(a)) sank into the B layer. Actually, the A-layer-V_{Fe} surface is the A termination layer with only half monolayer of Fe_{Tet} in the layer due to the Fe_{Tet} vacancy as shown in Fig. 2(b). Fe_{Oct} atoms in the surface layer exhibit a zigzag distortion along the y direction (Fig. 2(c)), which is similar to that in the SCV surface.[20] Note that on the surface, due to the low coordination, it is hard to say whether the Fe atom is tetrahedral or octahedral iron. In this case, the Fe atoms with magnetic moment in the same direction as Fe_{Tet} atoms are referred as Fe_{Tet} and the Fe atoms with magnetic moment in the same direction as Fe_{Oct} are referred as Fe_{Oct}.

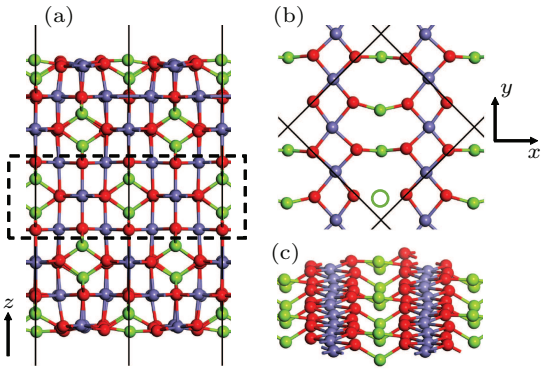


Fig. 2. Atomic structure of the A-layer-V_{Fe} model of Fe_3O_4 (001) surface: (a) side view, (b) top view with only the top two layers, (c) perspective view of the top two layers. The red, blue, and green balls represent O, Fe_{Oct}, and Fe_{Tet} atoms. Atomic layers in the dashed rectangles in panel (a) are kept fixed in the bulk positions during the atomic relaxation. The green circle in panel (b) denotes the Fe vacancy.

The geometry of other (001) surface models can be found in Figs. S1 and S2 in the supporting information. With oxygen vacancy, the B-layer exhibits two kinds reconstruction (Fig. S1). However, according to the calculated surface energy (solid and dashed green line in Fig. 1), the two kind of surfaces are not stable compared with SCV and A-layer-V_{Fe} surfaces for all possible μ_{O}. A complex reconstruction exists for the A layer (reconstructed A-layer, structure shown in Fig. S2), which can greatly reduce the surface energy (solid and dashed orange line in Fig. 1). However, the surface energy is still higher than that of SCV and A-layer-V_{Fe} surfaces.

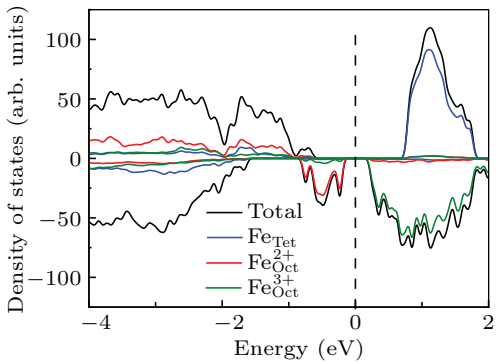


Fig. 3. Projected density of states (PDOS) on different Fe ions in the A-layer-V_{Fe} slab model. Legend of colors is on the top. The Fermi level is scaled to zero as indicated by the dashed black line.

Bader charge analysis[37,38] was performed to check the distribution of Fe^{2+} and Fe^{3+} in the A-layer-V_{Fe} slab model. Fe_{Tet} at the top surface layer is 2+ due to the low coordination and the other Fe_{Tet} ions are all 3+. Both Fe^{3+} and Fe^{2+} exist for Fe_{Oct} ions, which is similar to the case in bulk Fe_3O_4.[11] Projected density of states (PDOS) of the A-layer-V_{Fe} surface were calculated to investigate the electronic properties. According to the PDOS (Fig. 3), A-layer-V_{Fe} surface is a semiconductor with a band gap of 0.18 eV, which is much smaller

than the band gap of SCV (0.61 eV) and DBT (0.60 eV) surfaces.[22] Note that the calculated band gap of A-layer-V_{Fe} surface agrees well with the experimental value measured by scanning tunneling spectroscopy.[39] Similar to the DBT and SCV surfaces,[22] the band gap for spin down channel is between Fe^{2+} at octahedral sites (Fe^{2+}_{Oct}) and Fe^{3+} at octahedral sites (Fe^{3+}_{Oct}). According to the band decomposed charge densities, the valence band maximum (VBM) originates from Fe_{Oct} ions at both surface layers and inner bulk-like layers. The conduction band minimum (CBM) originates from Fe_{Oct} only at inner bulk-like layers.

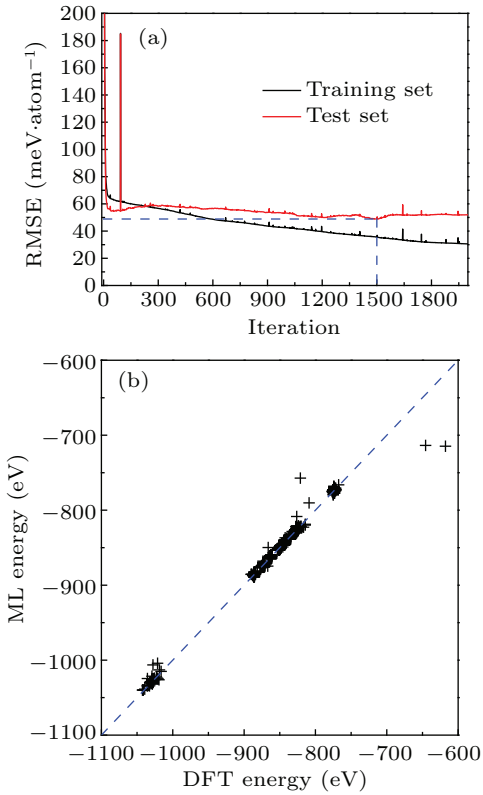


Fig. 4. (a) RMSE of the training and test sets as a function of training iteration. (b) Correlation of machine learning (ML) binding energies with the corresponding DFT reference energies for all structures in the testing sets. The blue dashed line indicates the condition that ML energy equals DFT energy.

The total magnetic moment (m_{tot}) of the A-layer-V_{Fe} model with 19 layers ($O_{72}Fe_{54}$) is 76 μ_B, *i.e.*, 1.407 μ_B per Fe atom, which is larger than the value for bulk Fe_3O_4 (1.333 μ_B per Fe). In bulk Fe_3O_4, all the Fe_{Tet} ions are 3+ and Fe^{2+}, Fe^{3+} at octahedral sites are half by half. In the A-layer-V_{Fe} model, Fe_{Tet} ions at the top surface layer are 2+, which leads to more Fe^{3+} than Fe^{2+} at octahedral sites according to the electroneutral condition. Therefore, the appearance of Fe^{2+}_{Tet} at the surface layer increases the m_{tot} according to the formula $m_{tot} = 5 \times [N(Fe^{3+}_{Oct}) - N(Fe^{3+}_{Tet})] + 4 \times [N(Fe^{2+}_{Oct}) - N(Fe^{2+}_{Tet})]$ proposed in our previous study,[40] where N is the number of the corresponding ions. For the SCV reconstruction, the model with 17 layers ($O_{72}Fe_{50}$) has a total magnetic moment of 64 μ_B, *i.e.*, 1.28 μ_B per Fe atom. Therefore, compare with the SCV reconstruction, the A-layer-V_{Fe} model has a larger m_{tot}.

Based on the data generated from DFT optimization of different Fe_3O_4 (001) surface models, we start to fit the Fe–O interaction by machine learning. A maximum of 2000 steps of error back propagation learning was performed, and 16898 (90%) data was used as the training set and 1877 (10%) data as the test set. The root-mean-square error (RMSE) of the test set was used to evaluate the training results. As shown in Fig. 4(a), after 1500 generations, the RMSE of the training set continues decreasing, while the RMSE of the test set start to increase. Therefore, over-fitting occurs after 1500 generations. The potential function obtained after 1500 generations of training is selected for subsequent calculations. The mean absolute error (MAE) and RMSE of the training set is 10.04 meV/atom and 35.56 meV/atom, respectively. The MAE and RMSE of the test set is 10.29 meV/atom and 48.89 meV/atom, respectively. For the test set, the corresponding relationship between the first-principles calculated total energies and the calculated value from the machine learning potential function is shown in Fig. 4(b). Most of the points in the test set fall well on the blue dashed line, implying the well performance of the machine learning.

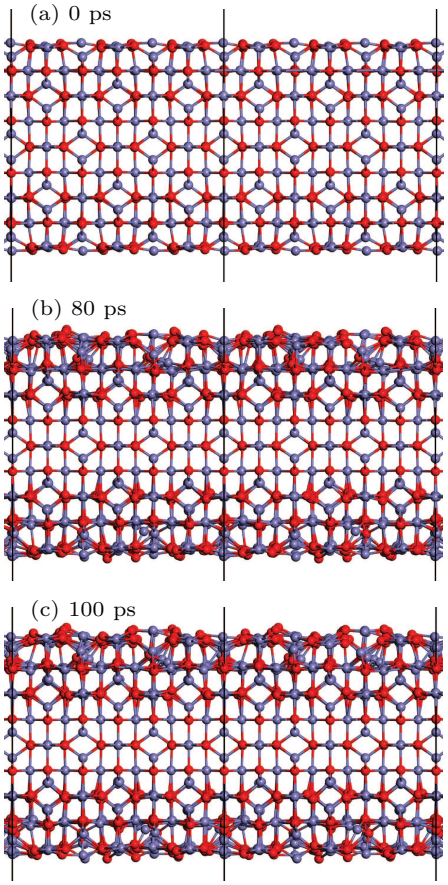


Fig. 5. Snapshot structures of the A-layer-V_{Fe} surface during molecular dynamics simulation at 400 K: (a) initial structure, (b) structure at 80 ps, (c) structure at 100 ps. The red and blue balls represent O and Fe atoms, respectively.

Based on the machine learning Fe–O interaction potential, an NVT molecular dynamics (MD) simulation at 400 K was performed to check the thermodynamic stability. A (3×3)

supercell of the A-layer-V_{Fe} surface model ($O_{648}Fe_{486}$) with a lattice parameter of 25.47 Å was used for the MD simulation. Snapshot structures are shown in Fig. 5. After 80 ps and 100 ps, the surface structure was well preserved though with some distortion. In the process of the synthesis of Fe_3O_4 nanoparticles in solutions[41–45] and in real applications of Fe_3O_4 nanoparticles in nanomedicine, the ambient temperature is lower than 400 K. Therefore, the A-layer-V_{Fe} surface is thermodynamically stable.

4. Conclusion

In summary, by the combination of DFT calculations, PSO method and machine learning, the possible reconstruction and stability of Fe_3O_4 (001) surface were systematically studied. Several different surface reconstruction models were obtained after five generation of PSO searching, including SCV, DBT, reconstructed A-layer, A-layer-V_{Fe}, A-layer-Fe adatom, B-layer-V_O-1, B-layer-V_O-2, and B-layer-V_{Fe}. Our results show that within a large range of oxygen chemical potential, SCV surface is the most stable surface. However, A-layer-V_{Fe} surface is also low in surface energy and at oxygen poor condition A-layer-V_{Fe} surface becomes more and more stable. Iron–oxygen interaction potential function was well fitted by machine learning. Base on the interaction potential function, MD simulation at 400 K was performed, which suggests that A-layer-V_{Fe} surface is thermodynamically stable. Our results provide atomic scale understanding of the reconstruction of Fe_3O_4 (001) surface and show the well performance of machine learning on the study of complex and magnetic metal oxides systems. In addition, our work is instructive for the study of surface reconstruction of other metal oxides.

Acknowledgements

Project supported by the National Natural Science Foundation of China (Grant Nos. 12004064, 12074053, and 91961204), the Fundamental Research Funds for the Central Universities (Grant No. DUT22LK11) and XingLiaoYingCai Project of Liaoning Province, China (Grant No. XLYC1907163). The calculations were performed on Tianjin Supercomputing Platform, Shanghai Supercomputing Platform.

References

[1] Mitchell M J, Billingsley M M, Haley R M, Wechsler M E, Peppas N A and Langer R 2021 *Nat. Rev. Drug Discov.* **20** 101
[2] Colombo M, Carregal-Romero S, Casula M F, Gutiérrez L, Morales M P, Böhm I B, Heverhagen J T, Prosperi D and Parak W J 2012 *Chem. Soc. Rev.* **41** 4306
[3] Chee H L, Gan C R R, Ng M, Low L, Fernig D G, Bhakoo K K and Paramelle D 2018 *ACS Nano* **12** 6480
[4] Sun S N, We C, Zhu Z Z, Hou Y L, Venkatraman Subbu S and Xu Z C 2014 *Chin. Phys. B* **23** 037503
[5] Li W Y, Li W T, Li B Q, Dong L J, Meng T H, Huo G, Liang G Y and Lu X G 2021 *Chin. Phys. B* **30** 104402
[6] Eerenstein W, Palstra T T M, Saxena S S and Hibma T 2002 *Phys. Rev. Lett.* **88** 247204
[7] Huang Z, Liu W, Liang J, Guo Q, Zhai Y and Xu Y 2022 *Chin. Phys. B* **31** 068505
[8] Zhu M and Wachs I E 2016 *ACS Catal.* **6** 722
[9] Sharma R K, Dutta S, Sharma S, Zboril R, Varma R S and Gawande M B 2016 *Green Chem.* **18** 3184
[10] Verwey E J W 1939 *Nature* **144** 327
[11] Liu H and Di Valentin C 2017 *J. Phys. Chem. C* **121** 25736
[12] Parkinson G S 2016 *Surf. Sci. Rep.* **71** 272
[13] Gaines J M, Bloemen P J H, Kohlhepp J T, Bulle-Lieuwma C W T, Wolf R M, Reinders A, Jungblut R M, van der Heijden P A A, van Eemeren J T W M, de Stegge J A and de Jonge W J M 1997 *Surf. Sci.* **373** 85
[14] Tarrach G, Bürgler D, Schaub T, Wiesendanger R and Güntherodt H J 1993 *Surf. Sci.* **285** 1
[15] Chambers S A, Thevuthasan S and Joyce S A 2000 *Surf. Sci.* **450** L273
[16] Mijiritskii A V and Boerma D O 2001 *Surf. Sci.* **486** 73
[17] Stanka B, Hebenstreit W, Diebold U and Chambers S A 2000 *Surf. Sci.* **448** 49
[18] Voogt F C, Fujii T, Smulders P J M, Niesen L, James M A and Hibma T 1999 *Phys. Rev. B* **60** 11193
[19] Pentcheva R, Wendler F, Meyerheim H L, Moritz W, Jedrecy N and Scheffler M 2005 *Phys. Rev. Lett.* **94** 126101
[20] Bliem R, McDermott E, Ferstl P, Setvin M, Gamba O, Pavelec J, Schneider M A, Schmid M, Diebold U, Blaha P, Hammer L and Parkinson G S 2014 *Science* **346** 1215
[21] Łodziana Z 2007 *Phys. Rev. Lett.* **99** 206402
[22] Liu H and Di Valentin C 2018 *Nanoscale* **10** 11021
[23] Novotny Z, Argentero G, Wang Z, Schmid M, Diebold U and Parkinson G S 2012 *Phys. Rev. Lett.* **108** 216103
[24] Wang P, Xing J, Jiang X and Zhao J 2022 *ACS Appl. Mater. Interfaces* **14** 33726
[25] Mao X, Wang L, Xu Y, Wang P, Li Y and Zhao J 2021 *npj Comput. Mater.* **7** 46
[26] Peng F, Sun Y, Pickard C J, Needs R J, Wu Q and Ma Y 2017 *Phys. Rev. Lett.* **119** 107001
[27] Zhong X, Wang H, Zhang J, Liu H, Zhang S, Song H-F, Yang G, Zhang L and Ma Y 2016 *Phys. Rev. Lett.* **116** 057002
[28] Shao G F, Zhu M, Shangguan Y L, Li W R, Zhang C, Wang W W and Li L 2017 *Chin. Phys. B* **26** 063601
[29] Sun Y and Hu W 2021 *SmartMat* **3** 474
[30] Sun Z, Yin H, Liu K, Cheng S, Li G K, Kawi S, Zhao H, Jia G and Yin Z 2022 *SmartMat* **3** 68
[31] Kresse G and Furthmüller J 1996 *Phys. Rev. B* **54** 11169
[32] Kresse G and Joubert D 1999 *Phys. Rev. B* **59** 1758
[33] Perdew J P, Burke K and Ernzerhof M 1996 *Phys. Rev. Lett.* **77** 3865
[34] Behler J 2011 *J. Chem. Phys.* **134** 074106
[35] Artrith N, Urban A and Ceder G 2017 *Phys. Rev. B* **96** 014112
[36] Reuter K and Scheffler M 2001 *Phys. Rev. B* **65** 035406
[37] Henkelman G, Arnaldsson A and Jónsson H 2006 *Comput. Mater. Sci.* **36** 354
[38] Sanville E, Kenny S D, Smith R and Henkelman G 2007 *J. Comput. Chem.* **28** 899
[39] Jordan K, Cazacu A, Manai G, Ceballos S F, Murphy S and Shvets I V 2006 *Phys. Rev. B* **74** 085416
[40] Liu H and Di Valentin C 2019 *Phys. Rev. Lett.* **123** 186101
[41] Sun S and Zeng H 2002 *J. Am. Chem. Soc.* **124** 8204
[42] Hou Y, Yu J and Gao S 2003 *J. Mater. Chem.* **13** 1983
[43] Sun S, Zeng H, Robinson D B, Raoux S, Rice P M, Wang S X and Li G 2004 *J. Am. Chem. Soc.* **126** 273
[44] Park J, An K, Hwang Y, Park J G, Noh H J, Kim J Y, Park J H, Hwang N M and Hyeon T 2004 *Nat. Mater.* **3** 891
[45] Tian Y, Yu B, Li X and Li K 2011 *J. Mater. Chem.* **21** 2476